Electromagnetic and pion-nuclear reactions on ^{15}N

C. Bennhold
TRIUMF, 4004 Wesbrook Mall, Vancouver, British,Columbia, Canada V6T 2A3

L. Tiator and S. S. Kamalov*
Institut für Kernphysik, Universität Mainz, 6500 Mainz, Germany

R. Mach
Institute of Nuclear Physics, Řež, Prague, Czecho-Slovakia Federal Republic
(Received 01 September 1992)

The effects of higher configurations in the ^{15}N wave function are studied in a variety of reactions, such as $^{15}N(e,e)^{15}$N, ^{15}N$(\gamma,\pi^-)^{15}$O$_{\rm g.s.}$ and ^{15}N$(\pi^+,\pi^0)^{15}$O$_{\rm g.s.}$. A (0+2)$\hbar\omega$ wave function for the $\mathcal{A}$=15 system that includes important contributions from the $(2s,1d)$ as well as $(2p,1f)$ orbitals modifies mostly the Fermi transitions and provides an improved description of the pion single charge exchange data on ^{15}N. The (γ,π^-) data require a wave function that can simultaneously fit the $M1$ form factor.
PACS numbers: 21.60−n, 25.20.Lj, 25.30.Bf, 25.80.Gn

I. INTRODUCTION

For over twenty years theoretical calculations have employed the matrix elements of Cohen and Kurath [1] as the nuclear structure input for reactions on p-shell nuclei. Their transition amplitudes were extracted from a global fit to energy spectra and static properties of a range of nuclei throughout the $1p$-shell using different forms for a phenomenological NN interaction. Their coefficients allowed for configuration mixing between the $1p_{1/2}$ and $1p_{3/2}$ orbits and, thus, the description of reactions was improved compared to using simple pure shell-model configurations. One serious drawback, however, was the restriction to the $1p$ shell only. A number of high-precision elastic and inelastic electron scattering experiments provided data [2–5] that could not be satisfactorily reproduced by using Cohen and Kurath amplitudes. Theoretical computations attempted to improve the situation by including contributions from core polarizations. As an alternative route, the nuclear structure coefficients were extracted by fitting them to the available observables, especially $M1$ form factors [3, 6–8], and then employing them to predict other reactions. In some cases the interpretation of these phenomenological coefficients in terms of a state vector has become questionable [9].

Recently nuclear structure calculations have become available [10] that pursue a description of nuclei with $\mathcal{A}$ = 4 – 16 within a full (0+2)$\hbar\omega$ shell model space. Thus, configuration mixing is not only restricted to the $1p$ shell, but includes contributions from the $2s$, $1d$, $2p$, and $1f$ shell as well. These wave functions achieve a good overall description of the relevant energy spectra. However, a recent criticism of this work [11] indicates that the parametrization of the effective two-body interaction used here differs from realistic interactions. This can lead to unphysical radial excitations in the low-lying spectrum in the case of ^{16}O nucleus. But as was pointed out in response to this critical point [12] only p-shell nuclei are well suited for treatment in the used model space. Their interaction should not be applied to describe states outside this model space, such as $0\hbar\omega$ states in the beginning of the sd shell and $1\hbar\omega$ states in the $1p$ shell.

The purpose of the present study is to investigate the significance of $2\hbar\omega$ configurations in ^{15}N in several reactions that involve the isovector transition to the isodoublet state ^{15}O$_{\rm g.s.}$, namely, ^{15}N$(J^\pi = \frac{1}{2}^-, T = \frac{1}{2}) \rightarrow ^{15}O(\frac{1}{2}^-, \frac{1}{2})$. The quantum numbers permit a spin-flip and non-spin-flip transition which in electromagnetic processes are the $M1$ and isovector $C0$ transitions, respectively. We will focus especially on the ^{15}N $M1$ electromagnetic form factor, π^- photoproduction, and pion single charge exchange since experimental data are available for all of the above reactions.

In recent calculations on processes involving ^{13}C it was shown that in particular the isovector $C0$ transition in photopion reactions is very sensitive to configurations outside the $1p$ shell [13]. Using a theoretical (0+2) $\hbar\omega$ shell model wave function reduced the $C0$ contribution to up to a factor of four and yielded good overall agreement with all available (γ,π^-) and (π^+,γ) measurements [14]. The largest effects of higher admixtures were found to be due to the $2p$ shell, followed by the $2s$ shell. Furthermore, the pion single charge exchange process ^{13}C$(\pi^+,\pi^0)^{13}$N$_{\rm g.s.}$ which is dominated by an isovector non-spin-flip potential revealed the significance of $2p$ shell admixtures as well [15].

In Sec. II of this work we will discuss different wave functions that have been employed for the $\mathcal{A} = 15$ system.

*Permanent address: Laboratory of Theoretical Physics, JINR Dubna, Head Post Office Box 79, SU-101000 Moscow, Russia.

 ©1992 The American Physical Society

Their predictions for the elastic $M1$ form factor will be compared to experimental data. Section III shows different results for the reaction $^{15}N(\pi^+,\pi^0)^{15}O$ in comparison with the available measurements. Much less data have been taken for the process $^{15}N(\gamma,\pi^-)^{15}O$ which is presented in Sec. IV. Finally, we summarize our findings in Sec. V.

II. THE ^{15}N $M1$ FORM FACTOR

In a pure shell model configuration the ground state of ^{15}N may be thought of as a $1p_{1/2}$ proton hole in a doubly-closed $1p$ shell. This can be seen in the experimental value of the magnetic dipole moment of ^{15}N which is -0.283μ_N and compares well with -0.263μ_N, the value for a $1p_{1/2}$ proton hole. The $\frac{3}{2}^-$ excited state at 6.32 MeV can be formed in this model by substituting a $1p_{3/2}$ hole for the $1p_{1/2}$ proton hole since the excitation energy of this state corresponds to the single-particle spin-orbit splitting in the $1p$ shell. Discrepancies between the experimental (e,e') form factors and the single proton hole description have to be interpreted as a contribution from multi-$\hbar\omega$ configurations [4] assuming that effects of non-nucleonic degrees of freedom, such as meson exchange currents (MEC) are small.

Figure 1 shows the experimental data for the $M1$ form factor in comparison with several calculations. The relevant nuclear structure matrix elements are defined in the LS-coupling scheme and can be found in Tables I, II, and III. The form factor computed in the single-proton-hole model appreciably exceeds the measured values around the maximum. At high momentum transfer Q the prediction decreases more rapidly than the experimental points; this phenomenon has been observed in $M1$ form factors of a number of other p-shell nuclei as well. We also present a calculation using the phenomenological wave function of Ref. [16] restricted to the $1p$ shell. In this model the $M1$ form factor is expanded in powers of $x = Q^2b^2/4$, b being the oscillator parameter and Q the momentum transfer, and the coefficients which contain the nuclear structure information are determined from a fit to the data. Only terms up to order x are present within the harmonic oscillator $1p$-shell space. Additional experimental input is given by the magnetic moment and the logft value which are included in the fit. The resulting amplitudes from Ref. [16] can describe the data well up to about 2.4 fm^{-1}. Note, however, that these reduced density matrix elements (RDME) would correspond to a ^{15}N wave function that does not fulfil the normalization condition.

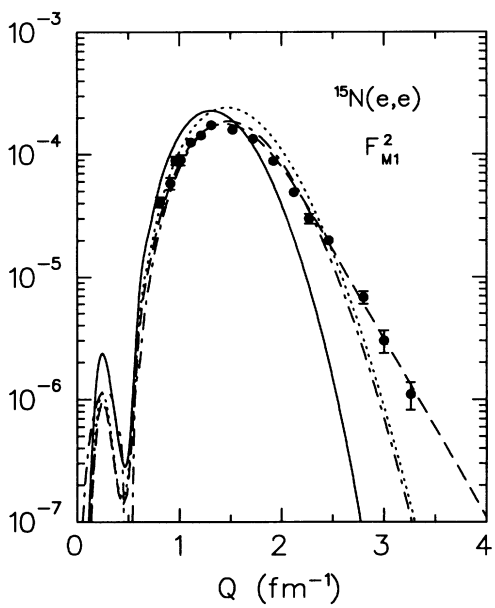

FIG. 1. The ^{15}N $M1$ form factor. The dotted curve was obtained with a pure hole wave function while the dash-dotted [full] curves were calculated with the $0\hbar\omega$ (Ref. [16]) [$(0+2)\hbar\omega$ (Ref. [10])] wave function. Dashed curve shows results obtained with the coefficients of Ref. [18]. The data are from Ref. [4].

TABLE I. ^{15}N nuclear structure matrix elements in the $0\hbar\omega$ model space. Note that $\psi_{1(11)} = 0$ and b =1.67 fm.

	J(LS) T=1			
$\psi_{J(\mathrm{LS});1}$	0(00)	1(10)	1(01)	1(21)
pure 1-hole	0.577	-0.471	0.192	-0.861
Ref. [16]	0.577	-0.437	0.179	-0.799

Measurements of $(e,e'p)$ cross sections in ^{16}O indicated that the occupancy of the $1p_{1/2}$ proton hole in the ground state of ^{15}N is only about 60% [17]. Recent theoretical shell-model calculations [10] in a $(0+2)\hbar\omega$ model space find similar results; the depletion is mainly attributed to contributions from 2p-2h excitations. In these calculations an effective empirical interaction is used that can be expressed in terms of 29 Talmi integrals. These integrals have been fitted to energy levels as well as magnetic dipole and electric quadrupole moments for $1p$-shell nuclei. For the $\mathcal{A}$=15 ground state the $T = 1,\ J = 0$ and $T = 1,\ J = 1$ transition matrix elements are listed in Table II. This wave function reproduces the ^{15}N mag-

TABLE II. $(0+2)\hbar\omega$ T=1 matrix elements for the $\mathcal{A}$=15 system from Ref. [10] with b=1.75 fm. Note that $\psi^{(n'\ell',n\ell)}_{J(\mathrm{LS})} = \psi^{(n\ell,n'\ell')}_{J(\mathrm{LS})}$ and that $\psi^{(n\ell,n'\ell')}_{1(11)} = 0$.

Configuration	J(LS) T=1			
$(n'\ell',n\ell)$	0(00)	1(10)	1(01)	1(21)
$(1p,1p)$	0.450	-0.370	0.162	-0.697
$(2p,1p)$	-0.122	0.008	-0.067	0.049
$(2p,2p)$	0.012	-0.007	0.009	-0.003
$(2s,1s)$	-0.069	–	-0.032	–
$(2s,2s)$	0.041	–	0.013	–
$(1d,1d)$	0.070	0.018	0.010	-0.011
$(1f,1f)$	0	0	0	0
$(1s,1d)$	–	–	–	-0.022
$(2s,1d)$	–	–	–	0.007
$(1p,1f)$	–	–	–	-0.054
$(2p,1f)$	–	–	–	0

TABLE III. The $T = 1$ nuclear structure coefficients for the $\mathcal{A}$=15 from Ref. [18] with b=1.23 fm.

Configuration	J(LS) T=1		
$(n'\ell', n\ell)$	1(10)	1(01)	1(21)
$(1p, 1p)$	-0.357	0.146	-0.651
$(2p, 1p)$	0.152	-0.062	0.277
$(3p, 1p)$	-0.082	0.033	-0.150
$(4p, 1p)$	0.025	-0.010	0.045
$(5p, 1p)$	-0.008	0.003	-0.015
$(2p, 2p)$	-0.065	0.026	-0.118
$(3p, 2p)$	0.035	-0.014	0.064
$(4p, 2p)$	-0.010	0.004	-0.019
$(3p, 3p)$	-0.019	0.008	-0.034
$(4p, 3p)$	0.006	-0.002	0.010

netic moment and the ^{15}O logft value fairly well; the theoretical results are -0.301μ_N and 3.637 compared to the experimental values -0.283μ_N and 3.63, respectively. The description of the $M1$ form factor, shown in Fig. 1, is unsatisfactory, especially at high Q where the theoretical prediction decreases much too rapidly. This is reminiscent of the situation in ^{13}C [14] and occurs for form factors of other p-shell nuclei as well [10]. A perfect description of the $M1$ form factor also at high Q can be obtained by performing a fit that permits higher powers of x. This has been done in Ref. [18], whose fit can be interpreted as an expansion of a single $1p_{1/2}$ proton hole wave function in terms of $1p$, $2p$, $3p$, $4p$, and $5p$ harmonic oscillator basis functions. The fitted oscillator parameter, b = 1.23 fm, is unusually small and indicates that it cannot be related to a nuclear charge radius. Thus, these nuclear structure coefficients (Table III) should be taken as a parametrization of the nuclear $J = 1$ transition densities but not as a ground state wave function of the $\mathcal{A}$=15 system that can be used to calculate other observables. Eventually, it would be desirable to perform shell-model calculations that include dynamical information such as form factors as a constraint.

We have not shown the isoscalar $C0$ form factor ($J = 0$ and $T = 0$) of ^{15}N here since both the full shell model wave function as well as a simple phenomenological $0\hbar\omega$ wave function can reproduce those data equally well as long as b is chosen to lie between 1.7 and 1.8 fm. The reason for this is the coherence effect in elastic charge form factors, where protons in all shells contribute coherently. This is in contrast to $M1$ form factors where only the valence nucleons contribute. Therefore, the effect of higher configurations in $C0$ form factors is reduced by roughly a factor of $1/Z$. Below we discuss charged pion photoproduction and pion single charge exchange where, due to an isospin flip, the coherence effect is not present as well.

III. PION SINGLE CHARGE EXCHANGE ON ^{15}N

The pion-nucleus interaction is described in the framework of multiple scattering theory, where the π-$\mathcal{A}$ scattering matrix $T(E)$ is obtained as a solution of the Lippmann-Schwinger equation [19]

$$T(E) = V(E) + V(E)P\mathcal{G}(E)T(E) \quad (1)$$

The pion-nucleus Green function is denoted by $\mathcal{G}$ (E), $V(E)$ stands for a potential matrix, and P is a projection operator which projects either on the nuclear ground state (optical model) or onto a group of nuclear states (coupled-channels model). In the latter case Eq. (1) is solved as a system of coupled equations. The potential matrix $V(E) = V_1(E) + V_2(E)$ can be divided into a first-order term $V_1(E)$ obtained via the impulse approximation, and a phenomenological term $V_2(E)$ that takes into account true pion absorption and higher-order processes. A detailed derivation of the potential matrix $V_1(E)$ which contains the full spin and isospin dependence of the pion-nucleon amplitudes can be found in Refs. [19–21].

In Fig. 2 we compare various calculations for the single charge exchange (SCE) process ^{15}N$(\pi^+, \pi^0)^{15}$O$_{g.s}$ with available experimental data at T_π = 48 MeV. Using the full (0+2)$\hbar\omega$ wave function of Ref. [10] rather than the amplitudes restricted to the $1p$ shell only [15] dramatically lowers the calculation at all angles improving the agreement with the measurements. This effect has already been observed in pion-nuclear reactions on ^{13}C, namely, ^{13}C$(\pi^+, \pi^0)^{13}$N [15] and ^{13}C$(\gamma, \pi^-)^{13}$N [14]. At smaller pion energies distortion effects are less significant, therefore the first term in Eq. (1) – which corresponds to the plane wave part – dominates the cross section. In this term the contributions from higher orbitals are added coherently to the usual terms from the $1p$ shell. However, since the large $2p$ shell amplitudes are of opposite sign to the $1p$ shell the resulting destructive interference lowers the calculated cross section.

Analyzing the angular distribution in Fig. 2 in more detail we note the additional minimum at backward an-

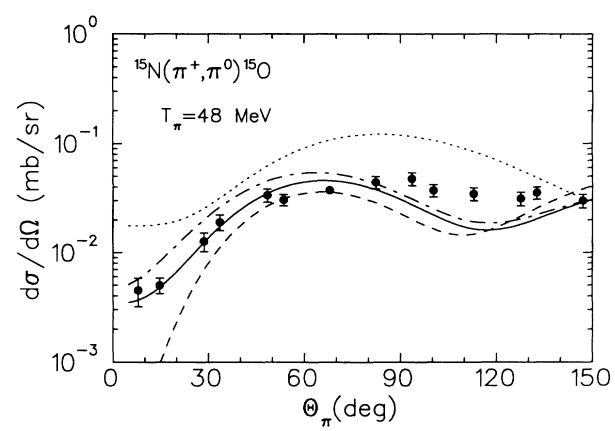

FIG. 2. Single charge exchange (SCE) ^{15}N$(\pi^+\pi^0)^{15}$O$_{g.s.}$ at T_π = 48 MeV. The dotted curve shows a calculation using the 0 $\hbar\omega$ wave function of Ref. [16]. The other three curves have been obtained with the (0+2)$\hbar\omega$ wave function of Ref. [10], the solid curve includes channel coupling to the $(\frac{3}{2}^-, \frac{1}{2})$ state in ^{15}N, the dash-dotted curve includes both the channel coupling and the true absorption term in the optical potential, and the dashed curve is obtained without channel coupling and true absorption. The data are from Ref. [22].

gles present in the calculations that use the $(0+2)\hbar\omega$ amplitudes. This is due to a minimum in the isovector $C0$ form factor at momentum transfer Q=1.1 fm^{-1}, caused by the higher configurations. Computing the same form factor within the $1p$ shell moves the minimum to Q=1.5 fm^{-1} which is outside the kinematical range for T_π =48 MeV. As shown in Fig. 3, the non-spin-flip part dominates the differential cross section almost everywhere, therefore, due to its isovector nature the (π^+, π^0) SCE process is ideally suited to study the $C0$ ($T = 1$) form factor. This effect is hidden in electron scattering because of the dominant $T = 0$ part which dominates the charge form factor. Due to the $C0$ dominance in the SCE process we have not performed calculations with the coefficients of Ref. [18] which were extracted from the $M1$ form factor.

At forward angles the plane wave part experiences a minimum due to the destructive interference between s and p waves in the elementary πN amplitudes. Therefore, the rescattering term, which is very sensitive to the nuclear model becomes important. Including the $2\hbar\omega$ admixtures, however, tends to weaken the effects of distortion and moves the full calculation closer to the plane wave result.

In the region of the destructive interference between the πN s and p waves, pion-nucleus cross sections can be very sensitive to the details of the scattering mechanism [22]. Since the ground state and the $(J^\pi, T) = (\frac{3}{2}^-, \frac{1}{2})$ (E_x = 6.23 MeV) state wave functions are very similar (i.e., in the pure shell model the $1p_{1/2}$ proton hole is replaced by the $1p_{3/2}$ hole), nuclear matrix elements of V_1(E) are expected to be larger in comparison to the analogous matrix elements for the transition to other excited states. Therefore, we believe that it is necessary to perform a coupled channels calculation in the model space containing both the ground and the $(\frac{3}{2}^-, \frac{1}{2})$ (E_x = 6.23 MeV) states. Employing the $(0+2)\hbar\omega$ wave function of Ref. [10] for the $\frac{3}{2}^-$ state we found the effects of this channel coupling to be important for small angles,

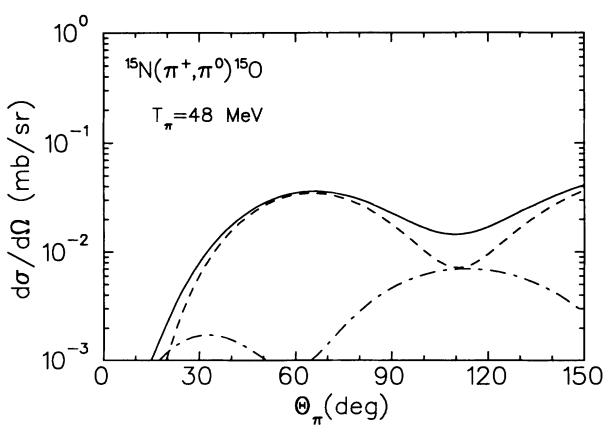

FIG. 3. The SCE process calculated with the $(0+2)\hbar\omega$ amplitudes without channel coupling or absorptive terms is shown by the solid curve. The dashed (dash-dotted) line shows the non-spin-flip (spin-flip) contribution separately.

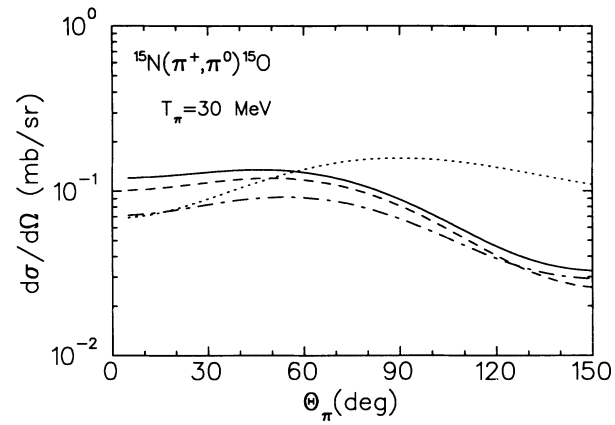

FIG. 4. Same as Fig. 2 for T_π = 30 MeV.

improving the description of the experimental data.

As shown in Fig. 4, the effects of including the excited nuclear states at T_π = 30 MeV is smaller since there is much less destructive interference between s and p waves. Only at larger angles, $\Theta_\pi > 80°$, the calculations using the $1p$ shell amplitudes and the $(0+2)\hbar\omega$ wave function differ for the reasons discussed above.

Figures 2 and 4 also present calculations that include the second-order optical potential $V_2(E)$ which is responsible for true pion absorption and other medium effects. This potential has been obtained phenomenologically from elastic π-nucleus scattering [21] on ^{12}C since little is known about its microscopic nature until now. From the results depicted in Fig. 2 and Fig. 4 we see that the sensitivity of the differential cross section to this ingredient is less than the sensitivity to the different nuclear structure input. Therefore, we believe that SCE on ^{15}N is a very good example to study the details of nuclear structure. Our results presented here show that simple $1p$ shell wave functions are not able to describe pion charge-exchange reactions. As in the case of the electromagnetic $M1$ form factor we find in this reaction, dominated by the isovector $C0$ transition, that, in the future, higher configurations have to be taken into account for ^{15}N nuclear wave functions.

IV. PION PHOTOPRODUCTION ON ^{15}N

While a lot of measurements at various momentum transfers and energies have been performed for the reaction ^{13}C$(\gamma, \pi^-)^{13}$N$_{g.s.}$ at several laboratories, very little experimental information is available for the process ^{15}N$(\gamma, \pi^-)^{15}$O$_{g.s.}$, the only experiments have been performed at low energy, E_γ = 170 MeV, at Mainz [16] and at Sendai [23].

Figure 5 compares the available data sets with calculations using various nuclear amplitudes for the $\mathcal{A}$=15 system. We perform our calculations in the framework of a momentum space DWIA; details can be found in Refs. [24] and [14]. Clearly the two experimental data sets from Mainz and Sendai are incompatible with each other. At forward angles all computations severely un-

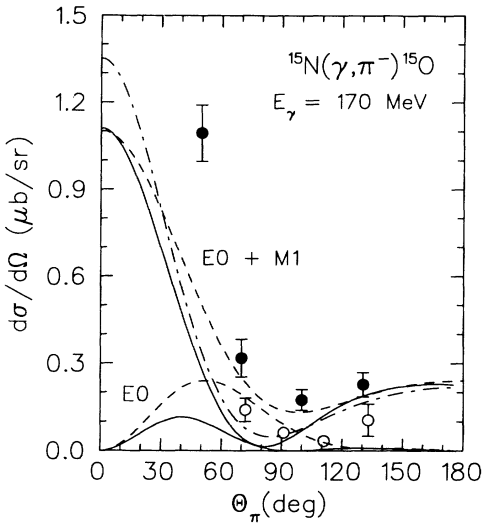

FIG. 5. The process ^{15}N$(\gamma,\pi^-)^{15}$O$_{g.s.}$ at $E_\gamma = 170$ MeV. The dashed curves are obtained with the $0\hbar\omega$ wave function of Ref. [16] and solid curves show the results obtained with the $(0+2)\hbar\omega$ wave function of Ref. [10]. The dash-dotted curve shows the $M1$ part only computed with the coefficients of Ref. [18]. The data are from Ref. [16] (solid circles) and Ref. [23] (open circles).

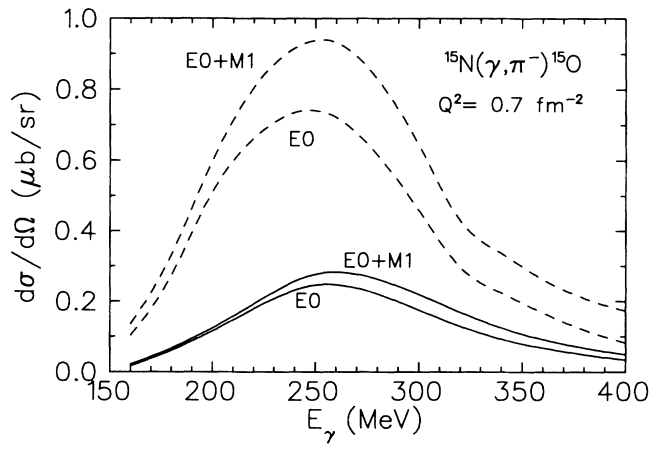

FIG. 6. As in Fig. 5 for $Q^2 = 0.7$ fm^{-2}.

derestimate the data point at Θ_π=50°. This is somewhat surprising since at forward angles – which corresponds to smaller momentum transfers – the $M1$ part in pion photoproduction is dominated by the $L = 0$, $S = 1$ matrix element, which in turn is constrained by the Gamow-Teller β decay. Note that at Θ_π=0° the effect of higher configurations is very small; due to orthogonality only diagonal configurations such as $(2s, 2s)$ or $(1d, 1d)$ can contribute. The calculation with the coefficients of Ref. [18] yields a significant enhancement at forward angles which is caused by the small harmonic oscillator parameter $b = 1.23$ fm. At larger angles the $1p$-shell wave function of Ref. [16] leads to a good description of the Mainz data while, on the other hand, the $(0+2)\hbar\omega$ amplitudes – similar to ^{13}C – lead to a reduction in the isovector $C0$ transition which is supported more by the Sendai data. The backward angle region is dominated by the $L = 2$, $S = 1$ part of the $M1$ transition; the small effects of higher configurations here is due to an accidental cancellation between the $(1s, 1d)$ and the $(1p, 1f)$ matrix elements.

Just as for the pion SCE we have not calculated the $C0$ transition with the coefficients of Ref. [18] since they do not reproduce the $C0$ charge form factor. As is evident from Fig. 6 no conclusions can be drawn until the experimental situation has been clarified. It is therefore imperative to perform new experiments soon, also at higher energies and for several momentum transfers [25]. In Fig. 6 we present calculations using the different wave functions at constant momentum transfer $Q^2 = 0.7$ fm^{-2}. At this Q^2 the $M1$ transition is very small, thus the cross section is dominated by the $C0$ transition. At higher Q^2 the $C0$ becomes negligible, measurements in this kinematic region may help to shed some light on the $M1$ matrix elements.

V. CONCLUSION

In this paper we have studied a number of electromagnetic and pion-nuclear reactions on ^{15}N comparing phenomenological wave functions with amplitudes obtained from $(0+2)\hbar\omega$ shell model calculations.

In electron scattering the effects of the higher configurations are negligible for the longitudinal form factor which is equally well described by either $0\hbar\omega$ or $(0+2)\hbar\omega$ amplitudes. The description of the transverse form factor is unsatisfactory with the $(0+2)\hbar\omega$ wave function, especially at higher momentum transfers. Here, clearly a pure phenomenological wave function as that given by Blok *et al.* [18] shows a perfect agreement with the data. However, the occupation numbers in the different harmonic oscillator shells differ considerably from the shell model calculations of Ref. [18]. A similar situation occurs for the $M1$ form factor of ^{13}C [10, 14]. At present it is not clear if these deviations stem from an effective interaction that is not optimal, a shell model space that is still too small, or other effects that have not been included [11].

The next reaction, pion single charge exchange on ^{15}N, is considerably better described when using the $(0+2)\hbar\omega$ amplitudes. In contrast to the $M1$ form factor this process is dominated by the non-spin-flip matrix elements. Thus complications with the $J = 1$ nuclear matrix elements as discussed above do not enter here. Including higher configurations as well as coupling to the $(\frac{3}{2}^-, \frac{1}{2})$ ($E_x = 6.23$ MeV) state improved the agreement between theory and experiment especially at lower pion energy where the angular distributions are very sensitive to nuclear structure.

Finally, we have compared calculations with differ-

ent wave functions to the two incompatible data sets of $^{15}N(\gamma,\pi^-)^{15}O_{g.s.}$. This reaction is very similar to $^{13}C(\gamma,\pi^-)^{13}N_{g.s.}$, where a $C0$ suppression could only be explained by higher configurations. In ^{15}N the $M1$ part which adds to the $C0$ incoherently is much stronger as in ^{13}C. Therefore, a nuclear wave function that reproduces – or fits – the $M1$ electromagnetic form factor is absolutely necessary. Upcoming experiments in Saskatoon at higher energies and different momentum transfers should provide more insight into this process.

ACKNOWLEDGMENTS

We are grateful to F. van Hees for providing us with the wave function of ^{15}N. One of the authors (S.S.K.) would like to thank R. Mach for the hospitality extended to him during his stay at the Institute of Nuclear Physics, Řež, Prague. This work was supported by the Deutsche Forschunsgemeinschaft (SFB 201) and the Natural Sciences and Engineering Research Council of Canada (NSERC).

[1] S. Cohen and D. Kurath, Nucl. Phys. **73**, 1 (1965); **A101**, 1 (1967).
[2] R. S. Hicks, J. Dubach, R. A. Lindgren, B. Parker, and G.A. Peterson, Phys. Rev. C **26**, 339 (1982).
[3] R. L. Huffman, J. Dubach, R. S. Hicks, and M. A. Plum, Phys. Rev. C **35**, 1 (1987).
[4] R. P. Singhal, J. Dubach, R. S. Hicks, R. A. Lindgren, B. Parker, and G. A. Peterson, Phys. Rev. C **28**, 513 (1983).
[5] T. W. Donnelly and I. Sick, Rev. Mod. Phys. **56**, 461 (1984).
[6] J. Dubach and W. C. Haxton, Phys. Rev. Lett. **41**, 1453 (1978).
[7] T. W. Donnelly and J. D. Walecka, Phys. Lett. **44B**, 330 (1973).
[8] M. K. Singham, Nucl. Phys. **A460**, 597 (1986); L. Tiator, Phys. Lett. **125B**, 367 (1983).
[9] K. Amos, D. Koetsier, and D. Kurath, Phys. Rev. C **40**, 374 (1989); I. Talmi, *ibid.* **39**, 284 (1989); C. Bennhold and L. Tiator, *ibid.* **42**, 464 (1990); D. Koetsier, K. Amos, L. Tiator, C. Bennhold, and L. E. Wright, *ibid.* **45**, 230 (1992).
[10] A. A. Wolters, A. G. M. van Hees, and P. W. M. Glaudemans, Phys. Rev. C **42**, 2053 (1990); **42**, 2062 (1990); A. G. M. van Hees, private communication.
[11] D. J. Millener, A. C. Hayes, and D. Strottman, Phys. Rev. C **45**, 473 (1992).
[12] A. A. Wolters, A. G. M. van Hees, and P. W. M. Glaudemans, Phys. Rev. C **45**, 477 (1992).
[13] C. Bennhold and L. Tiator, Phys. Lett. B **238**, 31 (1990).
[14] C. Bennhold and L. Tiator, Nucl. Phys. **A519**, 805 (1990).
[15] S. S. Kamalov, C. Bennhold, and R. Mach, Phys. Lett. B **259**, 410 (1991).
[16] A. Liesenfeld, B. Alberti, D. Eyl, G. Köbschall, A. W. Richter, K. Röhrich, Ch. Schmitt, L. Tiator, and V. H. Walther, Nucl. Phys. **A485**, 580 (1988).
[17] M. Bernheim *et al.*, Nucl. Phys. **A375**, 381 (1982).
[18] H. P. Blok and J. H. Heisenberg, in *Modern Topics in Electron Scattering*, edited by B. Frois and I. Sick (World Scientific, Singapore, 1991), p. 393; H. P. Blok, private communication.
[19] M. Gmitro, J. Kvasil, and R. Mach, Phys. Rev. C **31**, 1349 (1985).
[20] R. A. Eramzhyan, M. Gmitro, T. D. Kaipov, S. S. Kamalov, and R. Mach, J. Phys. G **14**, 1511 (1988).
[21] M. Gmitro, S. S. Kamalov, and R. Mach, Phys. Rev. C **36**, 1105 (1987).
[22] M. D. Cooper *et al.*, Phys. Rev. Lett. **52**, 1100 (1984).
[23] T. Kobayashi, K. Takeshita, A. Kagaya, H. Tsubota, and K. Shoda, J. Phys. Soc. Jpn. **58**, 1570 (1989).
[24] L. Tiator and L. E. Wright, Phys. Rev. C **30**, 989 (1984).
[25] T. Kobayashi *et al.*, Proposal for the Saskatchewan Accelerator Laboratory (SAL), 1991 (unpublished).